Resolution Enhancement Limitations for Spaceborne Scatterometers

Harrison Garrett

Brigham Young University

***Abstract*—The main limitation to the resolution enhancement of spaceborne scatterometers is the amplification of both measurement noise and model error. A few components to model error include: model discretization errors, interpolation errors, and the aliasing of frequency content introduced by each measurement spatial response function (MSRF). Using bandlimited reconstruction theory, we estimate the maximum resolution enhancement of a given sampling geometry through its inherent maximum square bandlimit. Simulations suggest that under bandlimited assumptions, the number of independent and uniformly distributed samples are proportional to the area of the sampling geometry's supported bandlimit. Furthermore, if we assume that the measurement noise is white Gaussian noise, then the supported bandlimit does not change. Using the simulations described in this paper, a rough estimate of the theoretical maximum resolution of a single swath of RapidScat 'egg' measurement is 5.55kmx5.55km.**

I. Introduction

Spaceborne scatterometers are essential tools for understanding the Earth's climate. Scatterometers use active radar sensors to measure the microwave backscatter reflected off the Earth's surface. Several important features of the Earth's climate can be derived from these measurements. For example, oceanic surface wind vectors can be inferred from scatterometer measurements. To this end, NASA has launched several scatterometer missions, which have all ended: NASA scatterometer (NSCAT), QuickScat, SeaWinds, and most recently RapidScat.

In an attempt to measure the entire surface of the Earth, most scatterometer measurement footprints cover a large area, which results in coarse measurement resolution. RapidScat's measurement footprint is about 16km wide with its measurement swath width being around 900km wide [1]. Many data products average measurements over a predefined grid, using a 'drop in the bucket' (DIB) technique. Products produced by DIB techniques are limited by the coarse resolution of individual measurement footprint areas. However, by taking advantage of the overlap between measurement footprints, resolution enhancement algorithms can resolve features smaller than each measurement footprint. For example, Stogryn enhanced radiometer measurements by applying the Backus Gilbert Inversion (BGI) method, and Long enhanced scatterometer measurements using the Scatterometer Image Reconstruction (SIR) algorithm [2], [3]. High resolution data products using RapidScat 'egg' measurements are subjectively enhanced to a 4.45km resolution grid and RapidScat 'slice' measurements on a 2.225km grid [4].

While it is known that resolution enhancement can increase the amount of resolvable features in scatterometer data products, the limitations of enhancement can be difficult to ascertain. The most apparent limitation to resolution enhancement is noise amplification. Most resolution enhancement algorithms are known to trade off improvements in spatial resolution with an increase in noise. The degree of enhancement is limited due to each algorithm's unique response to noise. For example, studies have shown that the SIR algorithm has

a smaller noise profile than BGI for similar gains in resolution, at least in the case of enhancing scatterometer measurements [5]. For most applications it is common to subjectively chose a resolution which appropriately balances both resolution enhancement and noise amplification. Due to the variation in noise amplification and resolution enhancing capabilities, it is difficult to determine the extent to which the resolution a particular scatterometer can be enhanced.

In order to better understand the limitations of scatterometer resolution enhancement, we briefly discuss some bandlimited reconstruction theory, some of the limitations of discrete estimation, and a basic approach to estimating the maximum square resolution supported by a particular sampling geometry. Then, using this approach, we roughly estimate the theoretical square maximum resolution inherent to RapidScat egg measurements.

II. Theory

A. Bandlimited Reconstruction

The theoretical max resolution should be solely based on a particular instrument's measurement geometry and sampling configuration. According to bandlimited reconstruction theory, the only type of surface a finite set of measurements can reconstruct is a bandlimited surface (i.e., a surface with a finite frequency response) [6]. In 1D sampling theory the Nyquist theorem assures us if the highest frequency in $f(t)$ is less than $2/T$, $f(t)$ can be fully represented by an infinite number of ideal samples $f[n] = f(nT)$:

$$f(t) = \sum_{-\infty}^{\infty} f[n]d(t - nT), \qquad (1)$$

where $f(t)$ is bandlimited function, $f[n]$ represents ideal samples of $f(nT) = f[n]$, and $d(t - nT)$ is the bandlimited identity function corresponding the the bandlimit of $f(t)$. A more finely spaced grid (a smaller T) corresponds to a higher bandlimit $(2/T)$.

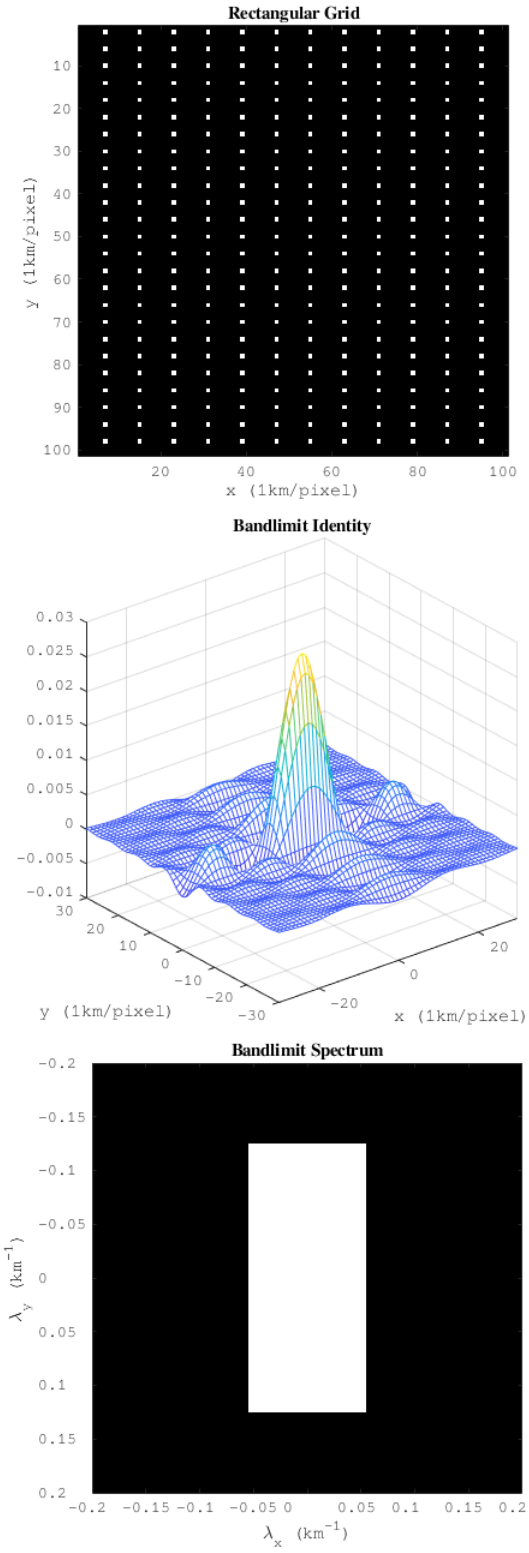

Fig. 1. Top, a rectangular sampling grid $\Delta x = 8$km, $\Delta y = 4$km. Middle, the corresponding maximum bandlimited identity function (the convolution of two Dirichlet kernels). Bottom, the maximum bandlimit's spectrum $1/\Delta x = 0.125\text{km}^{-1}$, $1/\Delta y = 0.25\text{km}^{-1}$ (λ_x: [-0.0625, 0.0625] km^{-1},λ_y: [-0.125, 0.125] km^{-1}.

When considering samples in 2D, the shape of the supported bandlimit depends on the sampling density and distribution. For example, a uniformly spaced rectangular grid with samples every Δx, Δy would have a rectangular region of support in the frequency domain with dimensions $1/\Delta x$, $1/\Delta y$ (see Fig. 1). Irregularly spaced samples may possess non-rectangular regions and spatial nulls in their spectrum of support. Instead of attempting to determine the spectrum shape that maximizes the 2D frequency content reconstructable from irregular samples, in this paper we simplify the estimation of a measurement geometry's supported bandlimit to its largest supported square bandlimit.

B. Discrete Estimation

In order to demonstrate the estimation of a sampling geometries maximum square bandlimit $d(t)$, we use a discrete 2D bandlimited reconstruction model:

$$f[k_j, l_j] = \sum_{i=1}^{N_i} a[x_i, y_i] d[x_i - k_j, y_i - l_j], \quad (2)$$

where $f[k_j, l_j]$ is an ideal sample of a bandlimited surface indexed by horizontal and vertical indices k_j and l_j respectively, N_i is the total amount of surface values $a[x_i, y_i]$ to reconstruct, $a[x_i, y_i]$ is each value of the bandlimited surface indexed by horizontal and vertical indices x_i and y_i respectively, and $d[x_i - k_j, y_i - l_j]$ is the discrete bandlimited identity corresponding to the bandlimit of $a[x, y]$ centered at $[k_j, l_j]$ and evaluated at $[x_i, y_i]$.

By placing the bandlimited surface $a[x_i, y_i]$ on a regularly spaced square grid with a separation of Δr, we can specify a reconstruction matrix $\mathbf{D}$ and vectorize Eq. 2:

$$\begin{aligned} \mathbf{f} &= \begin{bmatrix} f[1] & f[2] & \dots & f[N_j] \end{bmatrix}^T, \\ \mathbf{a} &= \begin{bmatrix} a[1] & a[2] & \dots & a[N_i] \end{bmatrix}^T, \\ \mathbf{D}_{ji} &= d[x_i - k_j, y_i - l_j], \\ \mathbf{f} &= \mathbf{D}\mathbf{s}, \end{aligned} \quad (3)$$

where $\mathbf{f}$ is a vector of ideal samples, N_j is the total number of ideal samples, $\mathbf{a}$ is a vector linearized into 1D indices $i = k + (l-1)N_i$ of surface values $a[x_i, y_i]$, N_i is the total number of values to reconstruct, $\mathbf{D}_{ji}$ is a matrix of bandlimited identity functions with dimensions $[N_j, N_i]$. The 2D DFT of $d[x, y]$ is known to be a square centered at zero with dimensions $[1/\Delta r, 1/\Delta r]$. In order to avoid indexing and discretization errors when computing the DFT, a 2D $[\sqrt{N_i}, \sqrt{N_i}]$ point FFT is used, where $\sqrt{N_i}$ is forced to be odd.

To reconstruct the surface $a[x_i, y_i]$, we must take the pseudo-inverse of $\mathbf{D}$:

$$\mathbf{a} = \mathbf{D}^\dagger \mathbf{f}, \quad (4)$$

where $\mathbf{D}^\dagger$ is the pseudo-inverse of $\mathbf{D}$. Note that although $d[x_i - k_j, y_i - l_j] = d[k_j - x_i, l_j - y_i]$, Eq. 2 can not be reversed (i.e., $\mathbf{D}^T\mathbf{f} \neq \mathbf{a}$, unless $\mathbf{D}$ is square and full rank).

In order to verify if a particular square bandlimit is supported by the ideal sampling in $\mathbf{f}$, we can create an error metric which checks Eq. 4:

$$e_b = \frac{1}{N_i} ||\mathbf{a} - \mathbf{D}^\dagger \mathbf{f}||^2, \quad (5)$$

where e_b is the bandlimited reconstruction error per pixel for a particular square bandlimit b.

C. Measurement Footprints

To incorporate samples with non-idealized measurement footprints, we modify the discrete bandlimited reconstruction case, by assuming that each measurement is accurately represented by:

$$z_j = \sum_{i=1}^{N_i} h_j[x_i, y_i] d[x_i - k_j, y_i - l_j] a[x_i, y_i], \quad (6)$$

where z_j is a non-idealized measurement, and $h_j[x_i, y_i]$ is the measurement spatial response function (MSRF) which represents how each

z_j was measured. By vectorizing $h_j[x_i, y_i]$ into 1D indices $i = k+(l-1)N_i$, we vectorize Eq.6:

$$\begin{aligned} \mathbf{z} &= \begin{bmatrix} z[1] & z[2] & ... & f[N_j] \end{bmatrix}^T, \\ \mathbf{H}_{ji} &= \begin{bmatrix} h_j[1] & h_j[2] & ... & h_j[N_i] \end{bmatrix}^T, \\ \mathbf{z} &= (\mathbf{H} \cdot \mathbf{D})\mathbf{a}, \end{aligned} \tag{7}$$

where $\mathbf{H}$ is the MSRF matrix with dimensions $[N_j, N_i]$, and $(\mathbf{H} \cdot \mathbf{D})$ denotes the element-wise multiplication of $\mathbf{H}$ and $\mathbf{D}$. Note that $(\mathbf{H} \cdot \mathbf{D})$ is equivalent to bandlimiting each $h_j[x_i, y_i]$ with the bandlimited identity of $\mathbf{a}$. To reconstruct $\mathbf{a}$ we must take the pseudo-inverse of the bandlimited $\mathbf{H}$:

$$\mathbf{a} = (\mathbf{H} \cdot \mathbf{D})^\dagger \mathbf{z}, \tag{8}$$

In order to verify if a particular square bandlimit is supported by the sampling in $\mathbf{z}$, we can create an error metric which checks Eq. 8:

$$e_b = \frac{1}{N_i} ||\mathbf{a} - (\mathbf{H} \cdot \mathbf{D})^\dagger \mathbf{z}||^2, \tag{9}$$

where e_b is the bandlimited reconstruction error per pixel for a particular square bandlimit b.

D. Discretization Errors

Since the discrete bandlimited reconstruction model used above assumes that $a[x_i, y_i]$ is the original discrete surface and measurement locations $[k_j, l_j]$ fall on the exact locations $[x_i, y_i]$, there is no MSRF discretization error in the above simulations. However, typical scatterometer measurements are modeled using the linear system:

$$z_j = \iint h_j(x, y) a(x, y) dx dy, \tag{10}$$

where $h_j(x, y)$ and $a(x, y)$ are continuous representations of $h_j[x_i, y_i]$ and $a[x_i, y_i]$ respectively. If $a(x, y)$ is assumed to be square bandlimited, then under bandlimited assumptions similar to Eq.6:

$$z_j = \iint h_j(x, y) d(x - k, y - l) a(x, y) dx dy, \tag{11}$$

where $d(x - k, y - l)$ is the continuous equivalent to $d[x_i - k_j, y_i - l_j]$. The relationship between $h_j[x_i, y_i] \neq h_j(x_i, y_i)$. Ideally, the discrete bandlimited verison of $h_j[x_i, y_i] = h_j(x_i, y_i) d(x - k, y - l)$. Mis-discretization of a bandlimited $h_j(x, y)$ contributes model error to the reconstruction process.

E. Interpolation Errors

Since real scatterometer measurements do not fall on a regular gird, in order to preform the maximum square resolution estimation on real data, measurement locations are interpolated onto a regular grid–contributing to model error. Another limiting aspect of this interpolating onto the $[\sqrt{N_i} x \sqrt{N_i}]$ Δr grid is quantization error. The 2D $[\sqrt{N_i}, \sqrt{N_i}]$ point FFT is limited to $1/(\sqrt{N_i}\Delta r)$ width bins when estimating the maximum supported bandwidth, so the estimate of the maximum resolution is quantized to the closest integer multiple of $1/(\sqrt{N_i}\Delta r)$.

III. Simulations

A. Ideal Sampling

To estimate the square maximum resolution of ideal sampling geometries, we simulate the ideal discrete bandlimited reconstruction case for two ideal grids with samples spaced $\Delta r_1 =$ 4km and $\Delta r_2 =$ 2km respectively (making $N_j = 625$ and $N_j = 2500$ respectively) over a discrete bandlimited image $\sqrt{N_i} =$ 101km. Additionally, to compare against irregular samples, random ideal non repeating samples are generated to match each N_j in each gridded case. Results are shown in Fig. 2, in which the maximum dimension of the square bandlimit corresponds to $1/\Delta r_1$ and $1/\Delta r_2$ respectively for gridded samples. Under the restriction that the random sampling is approximately uniformly distributed and samples are non repeating, the maximum supported bandlimit matches each gridded simulation.

This suggests that as long as measurements are uniformly distributed and independent, the

maximum resolution is proportional to $\sqrt{N_j}$. This assumption is supported by assuming that the rank of the bandlimited sampling matrix $\mathbf{D}$ is proportional to the maximum discrete square bandlimit's area.

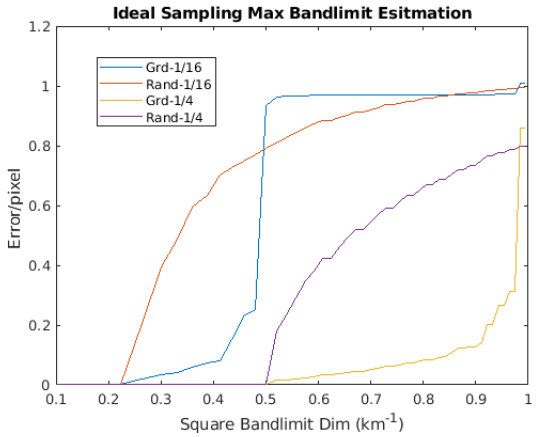

Fig. 2. The simulation results of bandlimited reconstruction error/pixel vs simulated square bandlimit areas. The 'Grd-1/4' and 'Grd-1/16' plots are spaced $\Delta r_1 = 4$km and $\Delta r_2 = 2$km respectively. The 'Rand-1/4' and 'Rand-1/16' plots are randomly space over a uniform distribution with the same N_j as in each Gridded simulations. The jump in error occurs respectively around .25km^{-1} and .5km^{-1}.

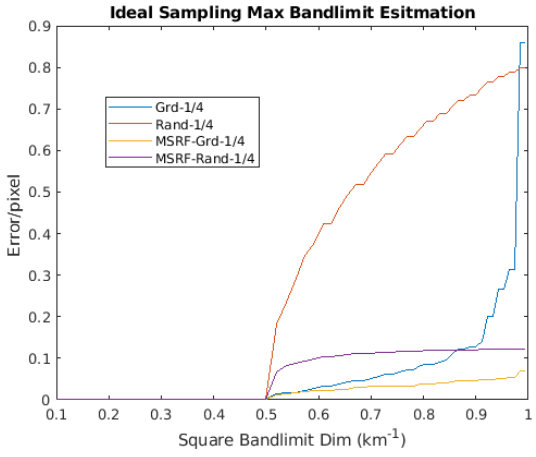

Fig. 3. Using random MSRFs, the bandlimited reconstruction error/pixel vs simulated square bandlimit areas is simulated. The 'Grd-1/4' and 'Grd-1/16' plots are spaced $\Delta r_1 = 4$km and $\Delta r_2 = 2$km respectively. The 'Rand-1/4' and 'Rand-1/16' plots are randomly space over a uniform distribution with the same N_j as in each Gridded simulations. The jump in error occurs respectively around .25km^{-1} and 0.5 km^{-1}.

B. Footprint Sampling

To test how non-ideal measurements with MSRFs compare to the ideal sampling case, we repeat the above simulations but include a randomly generated MSRF for each measurement. Results are shown in Fig. 3. The results indicate that the addition of MSRFs did not change the estimated maximum resolution. Instead, the reconstruction error/pixel past the maximum square bandlimit is noticeably lower when using MSRFs. This could be due to the Gaussian MSRFs acting as low pass filter on the accumulated reconstruction error.

C. Scatterometer Geometries

1) RapidScat Egg Measurements: For the RapidScat egg simulations, a square region over the Amazon was selected that covered the entire swath-width (specifically Latitudes $[-5°, 0°]$ and Longitudes $[-65°, -60°]$). Only measurements from a single ascending pass were selected (specifically those collected on Oct 27, 2015). In order to use the above simulation's format, measurements and MSRFs were interpolated onto a regular grid with 3.27kmx3.27km spacing. Measurements of poor instrument quality or invalid MSRFs were discarded in this simulation. The noise-free result is shown in Fig. 4, with a result of a maximum square bandlimit around 0.18km^{-1} square. The corresponding estimate of the theoretical maximum resolution for RapidScat egg measurements is 5.55kmx5.55km, with a quantization error around 0.1km in each dimension.

To visualize the effect of additive white Gaussian noise on the estimation of a RapidScat egg theoretical maximum resolution, the simulation described above was repeated with measurement noise added to the bandlimited measurements before reconstruction. The results using a various SNR levels are appended to the previous results and are shown in Fig. 5. Upon observation, it is apparent that for high SNR levels the theoretical maximum bandlimit did not change; however, for square bandlimit dimensions less than the supported bandlimit,

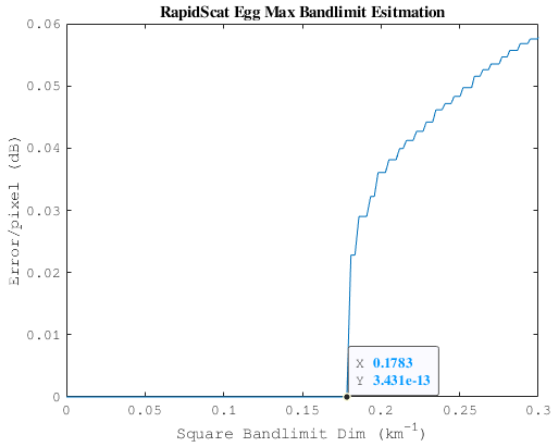

Fig. 4. Simulations using RapidScat egg measurements, which compare the bandlimited reconstruction error/pixel vs simulated square bandlimit areas. Samples were interpolated onto a 3.27kmx3.27km grid and over the Amazon (Latitude of $[-5°, 0°]$ and Longitude of $[-65°, -60°]$) using a single ascending pass. The jump in error occurs around 0.18km^{-1} corresponding to a theoretical maximum resolution of 5.55kmx5.55km.

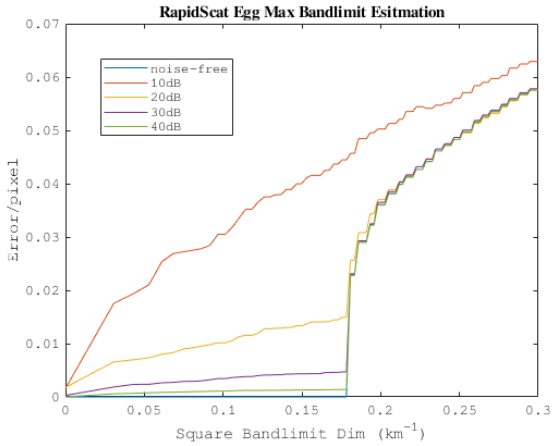

Fig. 5. Simulations incorporating additive white Gaussian measurement noise at SNRs=[10dB,20dB,30dB,40dB] using RapidScat egg measurements, which compare the bandlimited reconstruction error/pixel vs simulated square bandlimit areas. Samples were interpolated onto a 3.27kmx3.27km grid and over the Amazon (Latitude of $[-5°, 0°]$ and Longitude of $[-65°, -60°]$) using a single ascending pass. The jump in error (expect for the 10dB noise simulation) occurs around 0.18km^{-1} corresponding to a theoretical maximum resolution of 5.55kmx5.55km.

a baseline level of noise is observed. The amount of reconstruction error increases as the bandlimiting dimension is increased. This most likely because the bandlimit acts as a low pass filter on the cumulative reconstruction error. Note that at low SNR levels, the signal components of the image are overpowered by measurement noise, thereby making accurate reconstruction impossible.

The maximum resolution for a single swath of RapidScat egg measurements can be improved by aggregating multiple passes together. If we were to assume that the overlap of two RapidScat egg swaths double the amount of independent measurements–and additionally assuming that measurements are relatively uniformly distributed–we can roughly estimate the effective max resolution dimension of two aggregated swaths as half the resolution area of a single swath: $5.55\text{km}\sqrt{2} = 3.92\text{km}$. This result supports the resolutions tested in previous works, as the aggregate resolution is coarser than the resolution chosen for egg SIR images and finer than the resolution chosen for slice SIR images [4].

IV. Conclusion

The main limitation to the resolution enhancement of spaceborne scatterometers is the amplification of both measurement noise and model error. A few components to model error include: model discretization errors, interpolation errors, and the aliasing of frequency content introduced by each MSRF.

Typically, scatterometer resolution enhancement applications attempt to find a trade off between resolution enhancement and noise amplification specific to their chosen reconstruction algorithm. While this method is effective, it can be improved if we have and estimate of the theoretical maximum resolution. Using bandlimited reconstruction theory, we can find the maximum square resolution of a particular sampling geometry through an estimate of its inherent maximum square bandlimit.

Under bandlimited assumptions, our simulations show that the number of independent and uniformly distributed samples is proportional to the area of the sampling geometry's supported bandlimit. Additionally, if we assume that the

measurement noise is white Gaussian noise with a low SNR, then the supported bandlimit does does not change. Using the simulations described in this paper, a rough estimate of the theoretical maximum resolution of a single swath of RapidScat egg measurement is 5.55kmx5.55km.

Future work may revise these simulation to more efficiently and accurately estimate the bandlimited MSRF's pseudo-inverse, so that larger data sets and finer sampling grids can be used. Additionally, the results of these simulations can be validated by replacing the pseudo-inverse calculation with a resolution enhancement algorithm modified to be fully bandlimited.

REFERENCES

[1] S. L. Durden and D. Perkovic-Martin, "The Rapidscat Ocean Winds Scatterometer: A Radar System Engineering Perspective," *IEEE Geoscience and Remote Sensing Magazine*, vol. 5, no. 3, pp. 36–43, 2017.

[2] A. Stogryn, "Estimates of Brightness Temperatures from Scanning Radiometer Data," *IEEE Transactions on Antennas and Propagation*, vol. 26, no. 5, pp. 720–726, 1978.

[3] D. G. Long, P. J. Hardin, and P. T. Whiting, "Resolution Enhancement of Spaceborne Scatterometer Data," *IEEE Transactions on Geoscience and Remote Sensing*, vol. 31, no. 3, pp. 700–715, 1993.

[4] D. G. Long and B. R. Hicks, "Standard byu quikscat/seawinds land/ice image products," *Brigham Young University, Microwave Earth Remote Sensing Laboratory*, 2010.

[5] D. G. Long and D. L. Daum, "Spatial Resolution Enhancement of SSM/I Data," *IEEE Transactions on Geoscience and Remote Sensing*, vol. 36, no. 2, pp. 407–417, 1998.

[6] D. G. Long and R. O. W. Franz, "Band-limited Signal Reconstruction From Irregular Samples With Variable Apertures," *IEEE Transactions on Geoscience and Remote Sensing*, vol. 54, no. 4, pp. 2424–2436, 2016.